JOURNAL OF
Materials
CHEMISTRY

Synthesis and crystal structure of a new hydrated iron(III) vanadate $Fe_2(H_2O)[V_2O_7{\cdot}VO_3(OH)]$

Philippe Poizot,[a] Stéphane Laruelle,[a] Marcel Touboul,*[a] Michèle Louër[b] and Daniel Louër[b]

[a] *Laboratoire de Réactivité et de Chimie des Solides, UPRES-A 6007, Université de Picardie Jules Verne, 33 rue Saint-Leu, Amiens Cedex, France 80039.*
E-mail: marcel.touboul@sc.u-picardie.fr
[b] *Laboratoire de Chimie du Solide et Inorganique Moléculaire (UMR CNRS 6511), Cristallographie des Poudres et Réactivité des Solides, Université de Rennes 1, Avenue du Général Leclerc, Rennes Cedex, France 35042*

Received 17th January 2000, Accepted 16th May 2000
Published on the Web 27th June 2000

A new hydrated iron(III) vanadate was synthesized by an aqueous route from a V_2O_5 suspension in boiling water and iron(III) nitrate. The crystal structure of this well-crystallized yellow solid was solved *ab initio* from conventional X-ray powder diffraction data. The unit cell is orthorhombic with $a = 11.990(3)$, $b = 9.496(2)$, $c = 8.339(1)$ Å, $Z = 4$, space group $P2_12_12_1$. The refinement of 70 parameters by the Rietveld method, based on 1413 reflections, converged to the R-factors $R_F = 0.044$ and $R_{wp} = 0.097$. The structure of $Fe_2(H_2O)[V_2O_7{\cdot}VO_3(OH)]$ consists of a three-dimensional framework built from corner-sharing bi-tetrahedral V_2O_7 and independent tetrahedral $VO_3(OH)$ units interconnected with edge-sharing bi-octahedral $Fe_2O_9(H_2O)$ groups. A thermal study of this compound confirmed its water content and showed the existence of the corresponding anhydrous vanadate $Fe_2V_3O_{10.5}$, which provides, upon heating, a mixture of the two known iron(III) vanadates, namely the triclinic $FeVO_4$ and the $Fe_2V_4O_{13}$ phases.

Introduction

Only a few well characterized hydrated vanadates of trivalent elements have been reported in the literature, while a number of hydrated vanadates with divalent elements have been described.[1] For instance, compounds with the following chemical formulae have been found: $(AlOH)_3(VO_4)_2{\cdot}7.5H_2O$, $(AlOH)_2V_2O_7{\cdot}5H_2O$ and $Al_6V_{10}(OH)_{12}O_{28}{\cdot}29H_2O$,[2,3] $(ScOH)_2V_2O_7{\cdot}5.5H_2O$, $Sc_6O_4(OH)_4V_{10}O_{28}{\cdot}24H_2O$ and $Sc_5O_2(OH)_5V_{10}O_{28}{\cdot}25.5H_2O$,[4] $MVO_4{\cdot}nH_2O$ with M = Cr,[5] In,[6,7] Al,[8,9] Fe,[9–11] Y, Nd,[9] and Ga,[12] $M_4(V_2O_7)_3{\cdot}nH_2O$ with M = In,[7] Ga,[12] and Cr,[13] $M_2V_4O_{13}{\cdot}nH_2O$ with M = Fe,[1] Cr,[5] In,[6] Ga,[12] and Al,[14] $Cr(VO_3)_3{\cdot}nH_2O$,[15] $M_2V_{10}O_{28}{\cdot}nH_2O$ with M = Al, La, Nd, Er, and Yb,[16–19] $Cr(OH)V_{12}O_{31}{\cdot}nH_2O$,[20] $LnH_3V_{10}O_{28}{\cdot}nH_2O$;[21] with bismuth, three vanadates have been reported: $Bi_4V_6O_{21}{\cdot}6.5H_2O{\cdot}1.5NH_3$, $Bi_6V_2O_{14}{\cdot}3H_2O$ and $Bi_6V_4O_{19}{\cdot}6H_2O$.[22] Two of these compounds are minerals, steigerite ($AlVO_4{\cdot}3H_2O$)[8] and fervanite [$Fe_4(VO_4)_4{\cdot}5H_2O$],[10] which are characterized by their powder diffraction patterns. The structure of the decavanadates[16–19] has been determined. Some other compounds are amorphous to X-rays and are precursors of anhydrous vanadates, which are well characterized by indexed powder diffraction patterns, *e.g.* $CrVO_4$,[5] $InVO_4$,[6] $AlVO_4$, $FeVO_4$, YVO_4 and $NdVO_4$,[9] $Fe_2V_4O_{13}$,[1] $Cr_2V_4O_{13}$[5] and $In_2V_4O_{13}$.[6] The other compounds are only characterized by unindexed powder diffraction patterns, which does not permit confirmation of their existence as pure phases and, therefore, their chemical formula is questionable. These past few years, some vanadates of trivalent elements were found to be interesting candidates for anodes in lithium-ion batteries, especially the triclinic phase $FeVO_4$ and its amorphous precursor $FeVO_4{\cdot}2.7H_2O$.[23] To evaluate the electrochemical role of water in these compounds, we undertook a systematic synthesis of hydrated iron(III) vanadates. Until now, except for the mineral fervanite,[10] only amorphous hydrated iron(III) vanadates have been obtained, namely $FeVO_4{\cdot}2.7H_2O$[23] and $Fe_2V_4O_{13}{\cdot}4.4H_2O$.[1] In the present study, we describe the conditions for preparing a novel crystalline hydrated iron(III) vanadate. Due to the lack of single crystals, the structure was solved *ab initio* from X-ray powder diffraction data collected with a conventional X-ray source. In addition, the thermal behaviour of this phase is described.

Experimental

Synthesis

The compound was prepared by using a well-known solution-chemistry process, denoted method A.[1] For example, Tl_3VO_4 can be easily synthesized this way.[24] The general process involves maintaining a known amount of vanadium pentoxide as a suspension in boiling water over four hours. A nitrate (or chloride) solution containing the selected cation is then added in stoichiometric proportions. However, in our case, some adjustments were made in order to obtain the vanadate. Thus, the V_2O_5 activation stage was carried out over three days; the iron nitrate hydrate, $Fe(NO_3)_3{\cdot}9H_2O$, was then directly added. In this mixture the Fe : V ratio is equal to 1. The colour of the insoluble phase, initially orange, changed to yellow after 24 h of stirring and heating. After three additional days, the yellow precipitate was separated from the liquid phase, and washed with deionised water and with acetone. The solid phase was then dried at 50 °C in air for three days.

To determine the formula of the compound so-obtained, an analysis by EDS (energy dispersive spectroscopy) with a Link Isis, Oxford, apparatus was performed on several particles; a Fe : V ratio close to 2 : 3 was found. The water content was obtained by thermogravimetric analysis (see below), and was consistent with a content of three water molecules.

X-Ray powder diffraction

Precise X-ray powder diffraction data were collected with a Bruker AXS D5005 powder diffractometer using $CuK\alpha_1$–α_2 radiation ($\lambda K\alpha_1 = 1.5406$, $\lambda K\alpha_2 = 1.5444$ Å), selected with a

DOI: 10.1039/b000448k

Table 1 Details of the Rietveld refinement of $Fe_2(H_2O)[V_2O_7\cdot VO_3(OH)]$ (R values as defined in Langford and Louër)[33]

Formula weight/g mol^{-1}	459.532
Z	4
Density/g cm^{-3}	$Dx=3.21(1)$
Space group	$P2_12_12_1$ (no. 19)
2θ range/°	10–110
No. of atoms	17
No. of reflections	1413
No. of parameters	70
R_F	0.044
R_B	0.067
R_p	0.071
R_{wp}	0.097

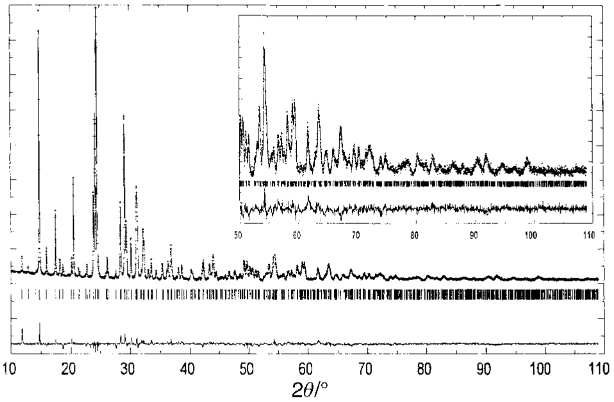

Fig. 1 Final Rietveld plot for $Fe_2(H_2O)[V_2O_7\cdot VO_3(OH)]$. The upper trace shows the observed data as dots and the calculated pattern is shown by the solid line. The lower trace is a plot of the difference: observed minus calculated. The vertical markers show the positions calculated for Bragg reflections. In the inset the intensity scale for the high-angle part of the pattern has been magnified by a factor of seven.

diffracted-beam graphite monochromator, using the parafocusing Bragg–Brentano geometry. The powder was mounted in a top-loaded sample holder[25] to minimize preferred orientation effects. The pattern of the compound was scanned over the angular range 10–110° (2θ) with a step length of 0.02° (2θ) and a counting time of 40 s step^{-1} up to 32.80° (2θ) and 80 s step^{-1} from 32.80° (2θ) to the end of the scan. The second range was then scaled to a counting time of 40 s step^{-1}. The peak position of individual diffraction lines was determined with the Socabim fitting program PROFILE, available in the PC software DIFFRACT-AT supplied by Siemens.

Thermal analyses

This compound was also characterized by thermal analyses using temperature-dependent X-ray powder diffraction, carried out with a Guinier-Lenné camera, operating with $CuK\alpha_1$ radiation. Experiments were performed under air with a heating rate of 0.1 °C min^{-1} up to 650 °C. TG–DTA measurements were performed with a Setaram TGDTA 92 instrument, using platinum crucibles, a heating rate of 10 °C min^{-1}, under air, and samples weighing about 20 mg.

Ab initio structure determination

Indexing

Indexing of the X-ray diffraction pattern was carried out by the successive dichotomy method using the program DICVOL91.[26] The first 20 lines were indexed on the basis of an orthorhombic cell with the figures of merit $M_{20}=68$ and $F_{20}=117(0.0045,38)$. The powder diffraction data available were reviewed with the program NBS*AIDS83,[27] from which the unit cell parameters were refined, and the space group $P2_12_12_1$ deduced from the systematic absences. From this evaluation the cell parameters were $a=11.990(3)$, $b=9.496(2)$, $c=8.339(1)$ Å, $V=949.4(2)$ Å^3, $Z=4$ [$M_{20}=57$, $F_{30}=76(0.0086,46)$]. The powder data will be submitted to the ICDD[28] for possible inclusion in the powder diffraction file.

Structure solution and refinement

Integrated intensities were extracted with the program EXPO[29] in the angular range 10–100° (2θ). Among the 600 reflections obtained, 198 were considered as statistically independent according to the degree of diffraction-line overlap. The structure-factor amplitudes thus obtained were used for the structure solution carried out with the direct-methods program available in the software package. A partial model corresponding to the lowest residual value (17%) was displayed, including 2Fe, 3V and 4O atoms in the asymmetric unit. These atomic coordinates were used in the program SHELXL-97[30] and several difference Fourier calculations showed the rest of the structure. A least-square Rietveld refinement with the program FULLPROF[31] was carried out in the angular range 10–110° (2θ) containing 1413 reflections. A pseudo-Voigt function was used to describe line profiles, with a variation of the mixing factor η as a linear function of the 2θ angle. As often observed with powder X-ray diffraction data,[32] some instabilities were encountered with the atomic displacement (thermal) parameters, particularly for the lighter atoms. Consequently, they were constrained to be equal for groups of identical atoms and then reasonable overall thermal parameters were obtained. The

Table 2 Final atomic coordinates and isotropic atomic displacement parameters (Å^2) of $Fe_2(H_2O)[V_2O_7\cdot VO_3(OH)]$, with esd's in parentheses (atomic displacement parameters were allowed to vary in the same manner for similar atoms)

Atom	x	y	z	B_{iso}
V(1)	0.7916(5)	−0.0831(7)	0.7065(8)	2.0(1)
V(2)	0.6147(5)	0.5754(6)	0.5022(11)	2.0(1)
V(3)	0.8971(5)	0.4958(6)	0.5017(13)	2.0(1)
Fe(1)	0.5259(6)	0.8148(8)	0.1895(12)	1.9(1)
Fe(2)	0.9738(6)	0.1955(8)	0.3056(12)	1.9(1)
O(1)	0.888(2)	−0.185(2)	0.830(3)	2.5(2)
O(2)	0.658(1)	−0.037(2)	0.781(3)	2.5(2)
O(3)	0.786(2)	−0.128(2)	0.485(2)	2.5(2)
O(4)	0.843(2)	0.100(2)	0.689(3)	2.5(2)
O(5)	0.752(1)	0.528(2)	0.483(3)	2.5(2)
O(6)	0.605(2)	0.622(3)	0.693(2)	2.5(2)
O(7)	0.519(1)	0.443(2)	0.517(4)	2.5(2)
O(8)	0.576(2)	0.690(2)	0.355(2)	2.5(2)
O(9)	1.149(2)	0.302(3)	0.284(4)	2.5(2)
O(10)	0.955(2)	0.581(3)	0.670(2)	2.5(2)
O(11)	0.971(2)	0.602(3)	0.372(2)	2.5(2)
O(12)	0.929(1)	0.316(2)	0.496(5)	2.5(2)

Table 3 Interatomic distances (Å) and angles (°) in $Fe_2(H_2O)[V_2O_7 \cdot VO_3(OH)]$[a]

VO_4 tetrahedra			
V(1)–O(1)	1.82(2)	O(1)–V(1)–O(2)	120(2)
V(1)–O(2)	1.77(2)	O(1)–V(1)–O(3)	117(2)
V(1)–O(3)	1.90(2)	O(1)–V(1)–O(4)	109(2)
V(1)–O(4)	1.85(2)	O(2)–V(1)–O(3)	111(2)
		O(2)–V(1)–O(4)	95(1)
mean	1.84(2)	O(3)–V(1)–O(4)	99(1)
V(2)–O(5)	1.71(1)	O(5)–V(2)–O(6)	103(2)
V(2)–O(6)	1.65(2)	O(5)–V(2)–O(7)	117(1)
V(2)–O(7)	1.71(2)	O(5)–V(2)–O(8)	111(2)
V(2)–O(8)	1.71(2)	O(6)–V(2)–O(7)	95(2)
		O(6)–V(2)–O(8)	120(2)
mean	1.70(2)	O(7)–V(2)–O(8)	110(2)
V(3)–O(5)	1.78(1)	O(5)–V(3)–O(10)	112(2)
V(3)–O(10)	1.76(2)	O(5)–V(3)–O(11)	110(2)
V(3)–O(11)	1.72(2)	O(5)–V(3)–O(12)	113(2)
V(3)–O(12)	1.75(2)	O(10)–V(3)–O(11)	92(2)
		O(10)–V(3)–O(12)	112(2)
mean	1.75(2)	O(11)–V(3)–O(12)	116(2)
FeO_6 octahedra			
Fe(1)–O(1^{i})	2.07(2)	O(1^{i})–Fe(1)–O(4^{ii})	170(2)
Fe(1)–O(4^{ii})	1.77(2)	O(1^{i})–Fe(1)–O(7^{iii})	94(2)
Fe(1)–O(7^{iii})	2.17(3)	O(1^{i})–Fe(1)–O(8)	87(2)
Fe(1)–O(8)	1.91(2)	O(1^{i})–Fe(1)–O(10^{iv})	90(2)
Fe(1)–O(10^{iv})	1.76(2)	O(1^{i})–Fe(1)–O(12^{ii})	78(2)
Fe(1)–O(12^{ii})	2.11(4)	O(4^{ii})–Fe(1)–O(7^{iii})	88(2)
mean	1.97(3)	O(4^{ii})–Fe(1)–O(8)	90(2)
		O(4^{ii})–Fe(1)–O(10^{iv})	100(2)
		O(4^{ii})–Fe(1)–O(12^{ii})	92(2)
O(7^{iii})–Fe(1)–O(8)	174(2)	O(8)–Fe(1)–O(10^{iv})	91(2)
O(7^{iii})–Fe(1)–O(10^{iv})	95(2)	O(8)–Fe(1)–O(12^{ii})	96(2)
O(7^{iii})–Fe(1)–O(12^{ii})	78(1)	O(10^{iv})–Fe(1)–O(12^{ii})	166(3)
Fe(2)–O(2^{v})	2.19(2)	O(2^{v})–Fe(2)–O(6^{ii})	101(2)
Fe(2)–O(6^{ii})	2.19(2)	O(2^{v})–Fe(2)–O(7^{vi})	80(2)
Fe(2)–O(7^{vi})	2.06(3)	O(2^{v})–Fe(2)–O(9)	160(2)
Fe(2)–O(9)	2.34(2)	O(2^{v})–Fe(2)–O(11^{vii})	82(2)
Fe(2)–O(11^{vii})	1.85(2)	O(2^{v})–Fe(2)–O(12)	106(2)
Fe(2)–O(12)	2.03(4)	O(6^{ii})–Fe(2)–O(7^{vi})	159(2)
mean	2.11(3)	O(6^{ii})–Fe(2)–O(9)	91(1)
		O(6^{ii})–Fe(2)–O(11^{vii})	101(2)
		O(6^{ii})–Fe(2)–O(12)	77(2)
O(7^{vi})–Fe(2)–O(9)	95(2)	O(9)–Fe(2)–O(11^{vii})	80(2)
O(7^{vi})–Fe(2)–O(11^{vii})	100(2)	O(9)–Fe(2)–O(12)	93(2)
O(7^{vi})–Fe(2)–O(12)	82(1)	O(11^{vii})–Fe(2)–O(12)	172(3)
Interconnection distances and angles			
V(1)–V(2^{viii})	4.23(2)		
V(1)–V(2^{ix})	4.25(2)		
V(1)–V(3^{x})	4.52(2)		
V(1)–V(3^{viii})	4.53(2)		
V(1)–Fe(1^{xi})	3.36(2)	V(1)–O(1)–Fe(1^{xi})	61(2)
V(1)–Fe(1^{vi})	3.67(2)	V(1)–O(1)–Fe(1^{vi})	141(2)
V(1)–Fe(2^{xiv})	3.46(2)	V(1)–O(2)–Fe(2^{xiv})	121(2)
V(2)–V(3)	3.47(2)	V(2)–O(5)–V(3)	168(2)
V(2)–Fe(1)	3.62(2)	V(2)–O(7)–Fe(1)	50(2)
		V(2)–O(8)–Fe(1)	177(2)
V(2)–Fe(1^{xii})	3.40(2)	V(2)–O(7)–Fe(1^{xii})	121(2)
		V(2)–O(8)–Fe(1^{xii})	64(2)
V(2)–Fe(2^{i})	3.47(2)	V(2)–O(6)–Fe(2^{i})	78(2)
		V(2)–O(7)–Fe(2^{i})	134(2)
V(2)–Fe(2^{xi})	3.50(2)	V(2)–O(6)–Fe(2^{xi})	131(2)
V(2)–O(7)–Fe(2^{xi})	55(2)		
V(3)–Fe(1^{xv})	3.50(2)	V(3)–O(10)–Fe(1^{xv})	169(2)
V(3)–O(12)–Fe(1^{xv})	44(2)		
V(3)–Fe(1^{xi})	3.46(2)	V(3)–O(10)–Fe(1^{xi})	67(2)
		V(3)–O(12)–Fe(1^{xi})	128(2)
V(3)–Fe(2)	3.41(2)	V(3)–O(11)–Fe(2)	61(2)
		V(3)–O(12)–Fe(2)	129(2)
V(3)–Fe(2^{xvi})	3.54(2)	V(3)–O(11)–Fe(2^{xvi})	165(2)
		V(3)–O(12)–Fe(2^{xvi})	45(2)
Fe(1)–Fe(2^{xiii})	3.20(2)		

[a] Symmetry code: (i): $x-1/2$, $1/2-y$, $1-z$; (ii): $1.5-x$, $1-y$, $z-1/2$; (iii): $1-x$, $y+1/2$, $1/2-z$; (iv): $x-1/2$, $1.5-y$, $1-z$; (v): $1.5-x$, $-y$, $z-1/2$; (vi): $x+1/2$, $1/2-y$,$1-z$; (vii): $2-x$, $y-1/2$, $1/2-z$; (viii): x, $y-1$, z; (ix): $1/2+x$, $1/2-y$, $1-z$; (x): $2-x$, $y-1/2$, $1.5-z$; (xi): $1.5-x$, $1-y$, $1/2+z$; (xii): $1-x$, $y-1/2$, $1/2-z$; (xiii): $1.5-x$, $1-y$, $z-1/2$; (xiv): $1.5-x$, $-y$,$1/2+z$; (xv): $1/2+x$, $1.5-y$, $1-z$; (xvi): $2-x$, $1/2+y$,$1/2-z$.

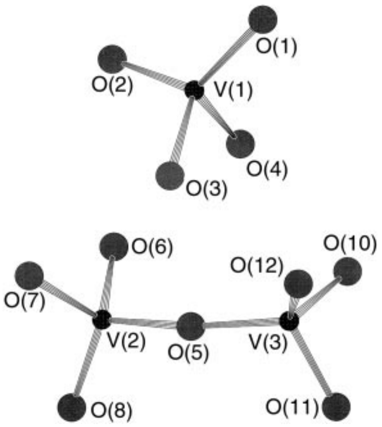

Fig. 2 View of the corner-sharing bi-tetrahedral V_2O_7 and tetrahedral $VO_3(OH)$ in $Fe_2(H_2O)[V_2O_7 \cdot VO_3(OH)]$.

refinement involved 54 atomic parameters (including 3 isotropic displacement parameters), 1 scale factor, 1 zero point, 3 cell parameters, 3 half-widths, 1 asymmetry parameter, 5 background polynomial parameters and the two parameters η and x characterizing the pseudo-Voigt function. The final refinement converged to the residual factors $R_F = 0.044$ and $R_{wp} = 0.097$. Details of the Rietveld refinement are given in Table 1 and final atomic coordinates in Table 2. Fig. 1 shows the best agreement obtained between calculated and observed patterns. Selected bond lengths and angles are listed in Table 3.

Description of the structure and discussion

From Table 3, it unambiguously appears that the three pentavalent vanadium ions are surrounded by a tetrahedron of oxygen atoms, and the two trivalent iron ions by an octahedron of oxygen atoms. The disposition of these polyhedra is particular. As O(5) is common to $V(2)O_4$ and $V(3)O_4$ tetrahedra, a divanadate (or pyrovanadate) ion, V_2O_7, exists (Fig. 2); the V(2)–O(5)–V(3) angle measures 168(2)° (Table 3). In this compound, two vanadate anions are present; a divanadate V_2O_7 and a vanadate VO_4. In the latter, corresponding to a $V(1)O_4$ tetrahedron, the longest V–O bond is V(1)–O(3); this oxygen atom probably belongs to a hydroxyl group to form a $VO_3(OH)$ group.

From Table 3, we can see that the oxygen atoms O(7) and O(12) belong to the two FeO_6 octahedra, $Fe(1)O_6$ and $Fe(2)O_6$; thus, these octahedra are linked together by their common edge O(7)–O(12) (Fig. 3). The longest Fe–O bond is Fe(2)–O(9); this oxygen atom, in an axial position in this octahedron, probably corresponds to the oxygen of a water molecule. Therefore, the structural formula of this new hydrated iron(III) vanadate(V) is: $Fe_2(H_2O)[V_2O_7 \cdot VO_3(OH)]$. The hypothesis considering O(3) as

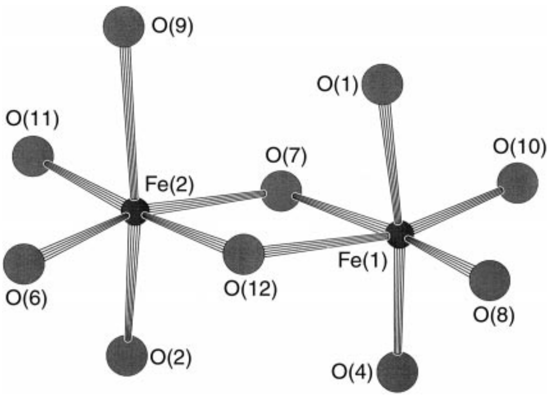

Fig. 3 View of the edge-sharing bi-octahedral $Fe_2O_9(H_2O)$ group in $Fe_2(H_2O)[V_2O_7 \cdot VO_3(OH)]$.

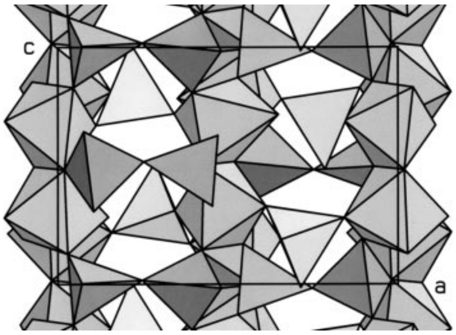

Fig. 4 Projection of the structure of $Fe_2(H_2O)[V_2O_7{\cdot}VO_3(OH)]$ on the (010) plane, showing the interconnection of groups forming a three-dimensional framework.

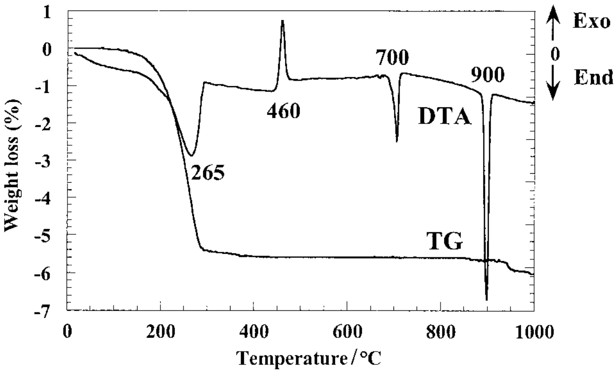

Fig. 6 TG and DTA curves of $Fe_2(H_2O)[V_2O_7{\cdot}VO_3(OH)]$, heating rate 10 °C min^{-1}.

an oxygen of a hydroxyl group and O(9) as an oxygen of a water molecule was confirmed when the linkage of all the VO_4 tetrahedra and the FeO_6 octahedra was determined. Thus, the $V(1)O_4$ tetrahedron is linked to the FeO_6 octahedra by three vertices O(1), O(2) and O(4); the fourth oxygen atom O(3) is free. The only O atom of the FeO_6 octahedra which is not common to the VO_4 tetrahedra or/and another FeO_6 octahedron is the oxygen O(9), which is bonded to Fe(2). Therefore, the structure of this compound consists of V_2O_7, $VO_3(OH)$ and $Fe_2O_9(H_2O)$ groups, which are linked together to form a three-dimensional network (Fig. 4). Tunnels parallel to the [001] direction exist in this structure, as shown in Fig. 5.

Such a complex vanadate ion is not common. To our knowledge, only one example has been reported for the cobalt-ethylenediamine-vanadate: $[Co(en)_3]^{3+}{}_2V_2O_7{}^{4-}HVO_4{}^{2-}\cdot 6H_2O$,[34] the structure of which was determined from single-crystal X-ray diffraction data. It is of interest to note that, in the cobalt compound, the values of the V–O distances in the VO_4 tetrahedra are between 1.594–1.817 Å, while in the iron vanadate, the distances are significantly longer, from 1.65 to 1.90 Å. In both cases, the longest distance corresponds to the bond of a vanadium atom with an oxygen of a hydroxyl group. These differences are probably due to the existence of isolated vanadate anions in the cobalt compound, where almost all the oxygen atoms are only bonded to vanadium atoms, while in the compound studied here they are also bonded to iron atoms.

Under atmospheric pressure, the structure of two iron(III) vanadates has been described, the triclinic $FeVO_4$[35] and $Fe_2V_4O_{13}$[36] phases. In the first compound, the Fe atoms have an octahedral and a trigonal bipyramidal environment, while in the second material the structure contains edge-sharing bi-octahedral Fe_2O_{10}, which can be compared with the $Fe_2O_9(H_2O)$ units existing in the vanadate studied here. The mean values of the Fe–O bonds are almost the same in the two compounds, 2.02 and 2.11 Å[36] instead of 1.97 and 2.11 Å (Table 3), even though the Fe–O distances range from 1.89 to 2.21 Å[36] instead of 1.76 to 2.34 Å here. In fact, the last distance corresponds to the Fe–OH_2 bond (Table 3).

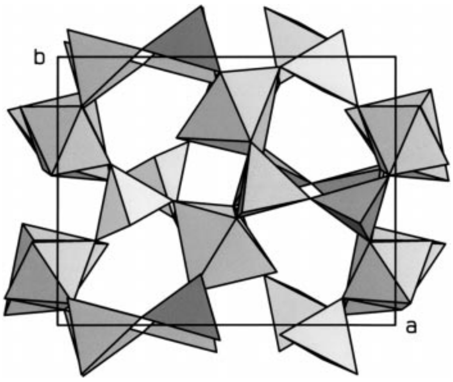

Fig. 5 Projection of the structure of $Fe_2(H_2O)[V_2O_7{\cdot}VO_3(OH)]$ on the (001) plane, showing tunnels parallel to the c direction.

Thermal properties

The thermogravimetric curve displayed in Fig. 6 shows that a weight loss starts from 120 °C and finishes around 280 °C. It corresponds to the content of water molecules in the formula of this compound (observed weight loss 5.65%, theoretical 5.87%). Simultaneously, a large endothermic effect is observed on the DTA curve. The three additional thermal effects appearing on this curve can be interpreted from both the results of the temperature-dependent X-ray diffraction photograph (Fig. 7) and the binary Fe_2O_3–V_2O_5 phase diagram.[37,38] In Fig. 7, the diffraction patterns have been attributed to $Fe_2(H_2O)[V_2O_7{\cdot}VO_3(OH)]$ up to 265 °C, where a new anhydrous phase with the formal composition $Fe_2V_3O_{10.5}$ appears. At about 415 °C, the main lines of the patterns of the two anhydrous iron vanadates $FeVO_4$ and $Fe_2V_4O_{13}$, which are stable phases in the Fe_2O_3–V_2O_5 phase diagram,[37,38] are observed. Around 650 °C, a partial melting of the solid occurs. A possible explanation of the thermal features on the DTA

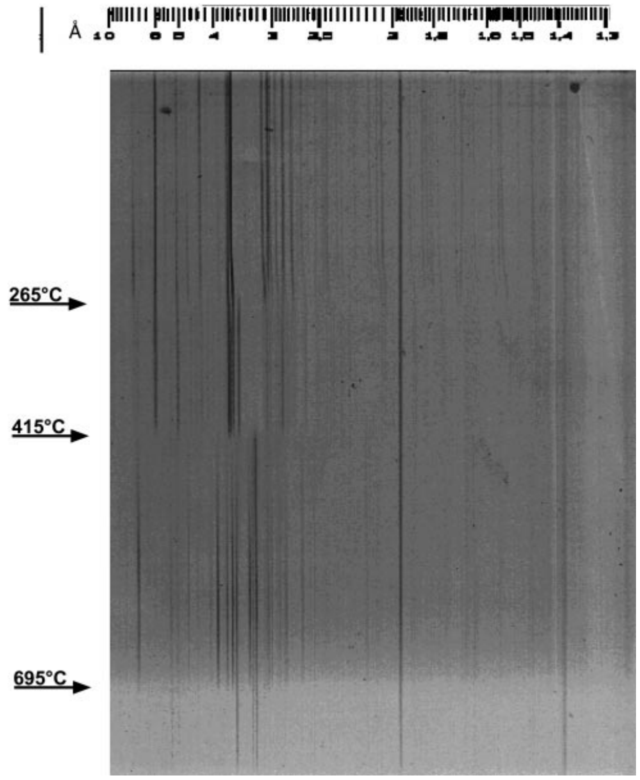

Fig. 7 Guinier–Lenné photograph of $Fe_2(H_2O)[V_2O_7{\cdot}VO_3(OH)]$, heating rate 0.1 °C min^{-1}.

curve can be proposed; the dehydration of the hydrated iron vanadate gives the new anhydrous crystalline vanadate $Fe_2V_3O_{10.5}$. The strong exothermic phenomenon at about 450 °C is likely due to the decomposition of this compound, which is not a stable phase in the Fe_2O_3–V_2O_5 binary system.[37,38] The next two endothermic effects, which are reversible, correspond to the two peritectic reactions of $Fe_2V_4O_{13}$ (67 mol% V_2O_5, 700 °C) and $FeVO_4$ (50 mol% V_2O_5, 900 °C) observed in the Fe_2O_3–V_2O_5 binary system[37,38] for the composition corresponding to the studied vanadate, 60 mol% V_2O_5. Powder diffraction data of the anhydrous phase were collected at room temperature from a sample prepared at 300 °C, and then cooled at room temperature. Although the quality of the diffraction data is moderate, the powder diffraction data were indexed by the program DICVOL91,[26] leading to the monoclinic solution: $a = 12.167(3)$, $b = 9.210(3)$, $c = 8.267(5)$ Å, $\beta = 95.95(4)°$, $V = 921.4(5)$ Å^3 [$M_{27} = 23$, $F_{27} = 51(0.0094,57)$]. The powder data will be submitted to the ICDD[28] for possible inclusion in the powder diffraction file. The cell parameters are somewhat related to those reported for the hydrated phase; however, attempts to solve the crystal structure from powder data were unsuccessful.

References

1 E. Baudrin, S. Denis, F. Orsini, L. Seguin, M. Touboul and J. M. Tarascon, *J. Mater. Chem.*, 1999, **9**, 101.
2 L. F. Chernysh, A. P. Nakhodnova and A. R. Makarova, *Russ. J. Inorg. Chem.*, 1979, **24**, 178.
3 A. A. Ivakin, M. V. Kruchinina, L. V. Chashchina, T. A. Denisova and O. V. Koryakova, *Russ. J. Inorg. Chem.*, 1991, **36**, 12.
4 L. V. Zaslavskaya, A. P. Nakhodnova and A. S. Mikhailova, *Russ. J. Inorg. Chem.*, 1979, **24**, 983.
5 M. Touboul and K. Melghit, *J. Mater. Chem.*, 1995, **5**, 147.
6 M. Touboul, K. Melghit and P. Bénard, *Eur. J. Solid State Inorg. Chem.*, 1994, **31**, 151.
7 L. F. Chernysh, A. P. Nakhodnova and L. V. Zaslavskaya, *Izv. Akad. Nauk SSSR, Neorg. Mater.*, 1976, **12**, 2009.
8 E. Ankinovitch, I. Kurmkaeva and I. Zazubina, *Zap. Vseross. Mineral. Ova.*, 1987, **116**, 100.
9 M. Touboul and A. Popot, *Rev. Chim. Miner.*, 1985, **22**, 610.
10 F. L. Hess and E. P. Henderson, *Am. Mineral.*, 1931, **16**, 273.
11 A. A. Ivakin, I. G. Chufarova, O. V. Koryakova, N. I. Petunina and L. A. Perelyaeva, *Russ. J. Inorg. Chem.*, 1980, **25**, 1817.
12 L. F. Chernysh, A. P. Nakhodnova and V. G. Pitsyuga, *Russ. J. Inorg. Chem.*, 1981, **26**, 1443.
13 D. Olivier and P. Rabette, *C. R. Hebd. Séances Acad. Sci.*, 1967, **265**, 1451.
14 A. P. Nakhodnova and L. F. Chernysh, *Ukr. Khim. Zh.*, 1976, **42**, 678.
15 J. Amiel, D. Olivier and M. Dessolin, *C. R. Hebd. Séances Acad. Sci.*, 1967, **264**, 1045.
16 G. Punte, B. E. Rivero, G. Rigotti and A. Navazza, *Acta Crystallogr., Sect. C*, 1988, **44**, 216.
17 B. E. Rivero, G. Punte, G. Rigotti and A. Navazza, *Acta Crystallogr., Sect. C*, 1985, **41**, 817.
18 B. E. Rivero, G. Rigotti, G. Punte and A. Navazza, *Acta Crystallogr., Sect. C*, 1984, **40**, 715.
19 Y. N. Saf'yanov, E. A. Kuz'min and N. V. Belov, *Kristallografiya*, 1979, **24**, 767.
20 M. V. Kruchinina, A. A. Ivakin, L. V. Chashchina, O. V. Koryakova and V. A. Kozlov, *Russ. J. Inorg. Chem.*, 1993, **38**, 705.
21 V. J. Sucha, *J. Therm. Anal.*, 1990, **36**, 1113.
22 P. K. Sinhamahapatra and S. K. Bhattacharyya, *J. Therm. Anal.*, 1979, **15**, 233.
23 S. Denis, E. Baudrin, M. Touboul and J. M. Tarascon, *J. Electrochem. Soc.*, 1997, **144**, 4099.
24 M. Touboul, M. Ganne, C. Cuche and M. Tournoux, *Z. Anorg. Allg. Chem.*, 1974, **410**, 1.
25 H. E. Swanson, M. C. Morris, E. H. Evans and L. Ulmer, *Nat. Bur. Stand., Monogr. (US)*, 1964, monogr. 25, sect. 3, p. 1.
26 A. Boultif and D. Louër, *J. Appl. Crystallogr.*, 1991, **24**, 987.
27 A. D. Mighell, C. R. Hubbard and J. K. Stalick, *NBS*AIDS83, A Fortran Program for Crystallographic Data Evaluation*, US Technical Note 1141, National Bureau of Standards, Washington, DC, 1981.
28 International Centre for Diffraction Data, Newtown Square, PA.
29 A. Altomare, M. C. Burla, M. Camalli, B. Carrozzini, G. L. Cascarano, C. Giacovazzo, A. Guagliardi, A. G. G. Moliterni, G. Polidori and R. Rizzi, *J. Appl. Crystallogr.*, 1999, **32**, 339.
30 G. M. Sheldrick *SHELXL-97, Program for Crystal Structure Refinement*, University of Göttingen, Göttingen, Germany 1997.
31 J. Rodriguez-Carvajal, in *Collected Abstracts of the IUCr Satellite Meeting on Powder Diffraction*, ed. D. Louër and J. Galy, Toulouse, France, 1990, p. 127.
32 L. B. McCusker, R. B. Von Dreele, D. E. Cox, D. Louër and P. Scardi, *J. Appl. Crystallogr.*, 1999, **32**, 36.
33 J. I. Langford and D. Louër, *Rep. Progr. Phys.*, 1996, **59**, 131.
34 S. Aschwanden, H. W. Schmalle, A. Reller and H. R. Oswald, *Mater. Res. Bull.*, 1993, **28**, 575.
35 B. Robertson and E. Kostiner, *J. Solid State Chem.*, 1972, **4**, 29.
36 L. Permer and Y. Laligant, *Eur. J. Solid State Inorg. Chem.*, 1997, **34**, 41.
37 A. A. Fotiev, S. M. Cheshnitskii and L. L. Surat, *Russ. J. Inorg. Chem.*, 1983, **28**, 560.
38 J. Walczak, J. Ziolkowski, M. Kurzawa, J. Osten-Sacken and M. Lysio, *Pol. J. Chem.*, 1985, **59**, 255.